

# SINGLE-CRYSTAL ELASTIC CONSTANTS OF MAGNESIUM AND MAGNESIUM ALLOYS\*

T. R. LONG† and CHARLES S. SMITH‡

The adiabatic elastic constants of single crystals of magnesium and dilute alloys of magnesium with Ag, In, and Sn have been measured by the ultrasonic pulse-echo technique. The values obtained for pure magnesium are:  $C_{11} = 0.597$ ,  $C_{33} = 0.617$ ,  $C_{44} = 0.164$ ,  $C_{12} = 0.262$ ,  $C_{13} = 0.217$ , all expressed in units of  $10^{12}$  dyne  $\text{cm}^{-2}$ . The alloy results show that within the experimental uncertainty all constants exhibit a smooth behavior as the electron concentration is increased to 2.020 per atom, through the critical region where zone overlap is thought to occur in the  $c$  direction. At most, a small change in slope could be read into the data for  $C_{11} + 2C_{33} + C_{12} - 4C_{13}$  at the critical electron atom ratio of 2.01. This behavior is in contrast to what might be expected from an extension of Leigh's predictions for the elastic constants of aluminium alloys.

## CONSTANTES ÉLASTIQUES DE MONOCRISTAUX DE MAGNÉSIUM ET D'ALLIAGES DE MAGNÉSIUM

Les constantes élastiques adiabatiques de monocristaux de magnésium et d'alliages de magnésium contenant de faibles teneurs en Ag, In, Sn, ont été déterminées par la technique d'écho ultra-sonore. Les valeurs obtenues pour le magnésium pur sont:  $C_{11} = 0.597$ ,  $C_{33} = 0.617$ ,  $C_{44} = 0.164$ ,  $C_{12} = 0.262$ ,  $C_{13} = 0.217 \cdot 10^{12}$  dyne  $\text{cm}^{-2}$ . Les résultats obtenus sur les alliages montrent, compte tenu des erreurs expérimentales, que toutes les constantes varient lentement lorsque la concentration électronique s'élève jusqu'à 2,020 par atome, à travers la région critique où l'on considère qu'il y a recouvrement de zones dans la direction  $c$ . Tout au plus un léger changement de pente peut être observé dans les résultats pour  $C_{11} + 2C_{33} + C_{12} - 4C_{13}$  au rapport critique électron/atome de 2,01. Ce comportement est en opposition avec ce que l'on pouvait attendre d'une extension des prédictions de Leigh pour les constantes élastiques des alliages d'aluminium.

## ELASTISCHE KONSTANTEN VON EINKRISTALLEN AUS MAGNESIUM UND MAGNESIUM-LEGIERUNGEN

Mit der Ultraschall-Puls-Echo-Methode wurden die adiabatischen elastischen Konstanten von Einkristallen aus Magnesium und verdünnten Legierungen von Magnesium mit Ag, In, und Sn gemessen. Die Messergebnisse für reines Magnesium sind:  $C_{11} = 0,597$ ,  $C_{33} = 0,617$ ,  $C_{44} = 0,164$ ,  $C_{12} = 0,262$ ,  $C_{13} = 0,217$ , alle in  $10^{12}$  dyn  $\text{cm}^{-2}$ . Die Ergebnisse an den Legierungen zeigen, dass alle Konstanten innerhalb der experimentellen Fehlergrenzen bei Zunahme der Elektronenkonzentration bis zu 2,020 Elektronen pro Atom einen glatten Verlauf aufweisen. Die gilt somit über den kritischen Bereich hinweg, in dem man damit zu rechnen hat, dass in  $c$ -Richtung die Elektronen in eine andere Brillouin-Zone übergreifen. Höchstenfalls war aus den Daten für  $C_{11} + 2C_{33} + C_{12} - 4C_{13}$  bei der kritischen Konzentration von 2,01 Elektronen pro Atom eine kleine Änderung im Anstieg abzulesen. Dieses Verhalten steht im Gegensatz zu den Erwartungen, die sich aus einer Verallgemeinerung der Leighschen Voraussagen für die elastischen Konstanten von Aluminiumlegierungen ergeben.

## INTRODUCTION

Lattice parameter measurements of magnesium alloys together with transport phenomena investigations by Schindler and Salkovitz<sup>(1)</sup> have shown the electronic structure of magnesium to be interesting with regard to Brillouin-zone overlaps. Fig. 1 shows the first zone for magnesium as deduced by Jones.<sup>(2)</sup> The smallest volume in  $k$  space bounded everywhere by an energy discontinuity is the Fig. 1-A bounded by  $A$ ,  $B$ , and  $C$  faces which contains sufficient volume for just 1.743 states per atom. Jones has added the six truncated prisms formed by an extension of the pyramidal faces  $C$ , so that 2 states per atom are available.

In the case of magnesium, overlap has already occurred across the  $A$  faces into the truncated prisms and across the edges marked  $Q$ , but not in the  $c$  direction across the  $B$  faces. Just the small addition of about 1 at. per cent of a trivalent alloy to magnesium is apparently enough to initiate the  $B$  overlap, as is illustrated in a plot of the  $c$  lattice parameter versus composition and in a recent measurement of the Hall constant as a function of composition by Schindler and Salkovitz.<sup>(1)</sup> The initiation of zone overlap is thought to cause rather abrupt changes in the Fermi energy of the crystal and thus it might be expected that there would be corresponding abrupt changes in the Fermi energy contribution to the elastic constants that would likewise show up in a plot of elastic constants versus composition. Leigh<sup>(3)</sup> has predicted such an effect with the  $(C_{11} - C_{12})/2$  shear constant in aluminum at an electron concentration of

\* Received June 27, 1956

† Formerly at Case Institute of Technology, Cleveland, Ohio. Now at Bell Telephone Laboratories, Murray Hill, New Jersey.

‡ Case Institute of Technology, Cleveland, Ohio.

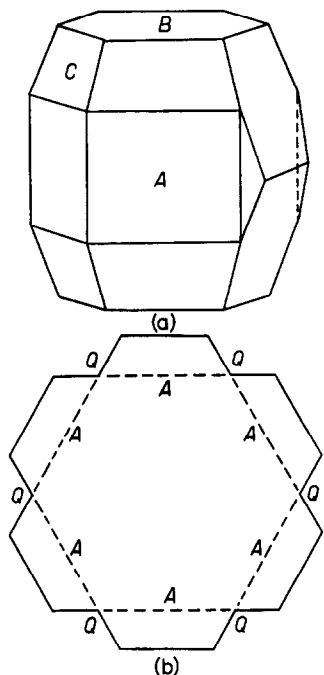


FIG. 1(a). The zone for Mg described by Jones, showing one of the six truncated prisms attached to an *A* face.

FIG. 1(b) Equatorial section of the complete zone.

2.67 per atom. At the present time there is no apparent way to test this expectation on aluminum alloy crystals, but since pure magnesium is very close to a similar critical point, knowledge of the behavior of the elastic constants of magnesium alloys as the electron concentration is increased through the critical region should be illuminating.

#### SAMPLE PREPARATION

Pure magnesium and several dilute alloys with tin, silver, and indium solutes were generously provided for this work by R. S. Busk of the Dow Chemical Company. The raw stock was always high-purity triply sublimed magnesium and correspondingly high-purity alloying material made up in the form of extruded alloy rods of 1-in. diameter. From these alloys as a starting point, single crystals in the form of a 1-in. diameter by 4-in.-long ingot were grown from the melt, using graphite crucibles. The crucible material was  $1\frac{1}{4}$ -in.-diameter AGX graphite rod obtained from the National Carbon Company of Cleveland, Ohio. These graphite rods were drilled and reamed with a reamer designed to put a  $\frac{3}{8}$ -in.-long, small-diameter, tapered nucleation tip on the end of an otherwise  $60^\circ$  conical tip. The crystal-growing furnace was a Lindberg Electric Globar furnace, modified to orient the combustion tube vertically and to allow the input power to be smoothly lowered at

any predetermined rate. The graphite crucible containing the magnesium was supported on the inside of the tube just below the center of the furnace by means of a  $\frac{1}{2}$ -in.-diameter by 8-in.-long copper rod which was threaded into the bottom of the crucible. The bottom end of this rod threaded into a water-cooled brass cap on the end of the combustion tube, and thus it also provided a heat-sink for establishing a large-temperature gradient in the melt. While growing the crystal, a helium atmosphere was maintained and the temperature lowered at the rate of about  $5^\circ\text{C}$  per hour. A complete growth cycle required approximately 2 days.

Those conditions which appear to be the most important for obtaining a high yield of single crystals are: first, the establishment of a large ( $7^\circ\text{C}/\text{cm}$ ) temperature gradient in the crucible; second, superheating of the molten material by as much as  $200^\circ$  before dropping the temperature to just above the melting-point and starting the slow cool; and third, the presence of a nucleation tip on the crucible. For this furnace, the slow cooling was necessary to obtain the alloy single crystals, but other materials such as Cu, Ag, Al, and pure Mg have been grown successfully at cooling speeds of  $1^\circ\text{C}/\text{min}$ .

Chemical analyses of thin slabs cut from the large crystal just above and below the section used for the measurements were made by the James H. Herron Company of Cleveland. All of the alloys showed a longitudinal concentration gradient larger than that observed for copper and silver alloys in this laboratory, with the highest concentration at the top of the ingot. An average value of the two compositions thus obtained was used, since the bulk value of concentration is the important quantity for this work.<sup>(4)</sup> In addition, densities obtained by hydrostatic weighing on five of the samples were in excellent agreement with the values calculated from chemical analysis and lattice parameter data. The density is a sensitive function of composition in these alloys. Spectrographic analyses of pure magnesium crystals showed them to be at least 99.99% pure.

The crystals in just the condition as they came out of the furnace showed brilliant flash planes which made the identification and orientation of single crystals simple. An optical goniometer was designed in which reflections from the crystal fell on a curved screen. For magnesium, the  $\{10\bar{1}0\}$ ,  $\{10\bar{1}1\}$ , and  $\{0001\}$  planes give well-defined reflections. The procedure for optically orienting the crystals consisted of adjusting the crystal until a symmetrical equatorial pattern of spots was observed. Azimuth angle measurements identified the reflections, and

then further goniometer readings of the appropriate angles yielded orientations good to 1 deg. Optical orientations were used for determining where and how the crystal should be cut for measurements, but, after the measurements had been completed on a given sample crystal, final orientations were measured by the back-reflection Laue and stereographic projection techniques. These final orientations are good to half a degree.

Conventional techniques for cutting the crystals to the proper orientation for measurements produced more cold work in magnesium than was deemed tolerable for single-crystal measurements. For this reason an acid saw was used. It consisted of a No. 30 mercerized cotton crochet thread belt which passed over a pulley dipped in acid and thence across the sample. A small, inexpensive lathe was used to advance the sample past the string. With a string speed of 75 ft per minute and a 15% solution of HCl in water, quite satisfactory cuts were made on the 1-in. sample in about 3 hours. The surfaces obtained from the saw were flat to 4 mils, but it seems probable that still better results could be obtained with more experimentation.

After cutting, the single-crystal samples were waxed into 2½-in.-diameter steel lapping rings and given a metallographic polish through 3/0 paper. About 5 mils were removed from each side in this process, yielding surfaces which were flat and parallel to 0.0001 in.

#### ACOUSTIC MEASUREMENTS

The pulsed ultrasonic technique was used to obtain acoustic-wave velocities in various crystallographic directions in the sample. The actual calculation of the elastic constants from the wave velocities was done by means of a perturbation technique developed by Neighbours.<sup>(5)</sup> The pertinent relationships between acoustic-wave velocity and elastic constants of hexagonal crystals are reproduced here:

$$\left. \begin{aligned} C'_{11}(l, m, n, C_{ij}) &= \rho V_1^2 - \left\{ \frac{C'_{15}}{C'_{11} - C'_{55}} \right\} \\ C'_{66}(l, m, n, C_{ij}) &= \rho V_2^2 \\ C'_{55}(l, m, n, C_{ij}) &= \rho V_3^2 + \left\{ \frac{C'_{15}}{C'_{11} - C'_{55}} \right\} \end{aligned} \right\} \quad (1)$$

Here  $l, m, n$  are the direction cosines of the direction of propagation,  $C_{ij}$  are the elastic constants of the crystal referred to the conventional reference axes,  $C'_{ij}$  are the elastic constants referred to another coordinate system with the  $X$  axis along the direction of propagation,  $\rho$  is the density, and  $V_1, V_2,$  and  $V_3$

refer respectively to the velocities of a longitudinal wave and two shear waves propagated along  $X$ . For the hexagonal system, the primed elastic constants are related to the unprimed elastic constants by the relations:

$$C'_{11} = \alpha^4 C_{11} + 2n^2 \alpha^2 C_{13} + n^4 C_{33} + 4n^2 \alpha^2 C_{44} \quad (2)$$

$$C'_{66} = \alpha^2 \left( \frac{C_{11} - C_{12}}{2} \right) + n^2 C_{44} \quad (3)$$

$$C'_{55} = n^2 \alpha^2 C_{11} - 2n^2 \alpha^2 C_{13} + n^2 \alpha^2 C_{33} + (\alpha^2 - n^2)^2 C_{44} \quad (4)$$

$$C'_{15} = -n\alpha^3 C_{11} + n\alpha(\alpha^2 - n^2) C_{13} + n^3 \alpha C_{33} + 2n\alpha(\alpha^2 - n^2) C_{44} \quad (5)$$

$$\text{where} \quad \alpha^2 = l^2 + m^2. \quad (6)$$

To obtain values for the five unprimed elastic constants in equation (2) through (5), one must measure at least five independent wave velocities.

Note that in the above equations, if the direction of propagation is perpendicular to the  $c$  axis of the crystal, then  $n^2 = 0, \alpha^2 = 1$ , and we have

$$\left. \begin{aligned} C'_{11} &= C_{11} = \rho V_1^2 \\ C'_{55} &= (C_{11} - C_{12})/2 = \rho V_2^2 \\ C'_{66} &= C_{44} = \rho V_3^2 \\ C'_{15} &= 0 \end{aligned} \right\} \quad (7)$$

so a longitudinal wave propagated in the basal plane determines  $C_{11}$  directly, a shear wave propagated in the basal plane with particle motion also in the basal plane determines  $(C_{11} - C_{12})/2$ , and a shear wave with particle motion along the  $c$  axis determines  $C_{44}$ .

$C_{33}$  could be determined directly by a longitudinal-wave velocity directed along the  $c$  axis ( $n^2 = 1, \alpha^2 = 0$ ), but  $C_{13}$  could not be determined by any wave propagated in this direction, since both shear waves in this direction measure  $C_{44}$ . Thus, to measure all 5 elastic constants, the sample crystal was cut and oriented as shown in Fig. 2.

The velocities of the waves shown are sufficient to completely determine the elastic constants of a hexagonal material.  $V_4, V_5,$  and  $V_6$  determine  $C_{11}, (C_{11} - C_{12})/2,$  and  $C_{44}$  directly, as stated above. Then, having these values,  $V_1$  and  $V_3$  taken together provide a determination of  $C_{33}$  and then either  $V_1$  or  $V_3$  allows a determination of  $C_{13}$ .  $V_2$  provides nothing new, since  $\rho V_2^2$  is just a combination of  $(C_{11} - C_{12})/2$  and  $C_{44}$ , both of which are better measured by  $V_5$  and  $V_6$ .

In the pulsed ultrasonic technique used in these measurements a 10-megacycle quartz ( $X$  cut for

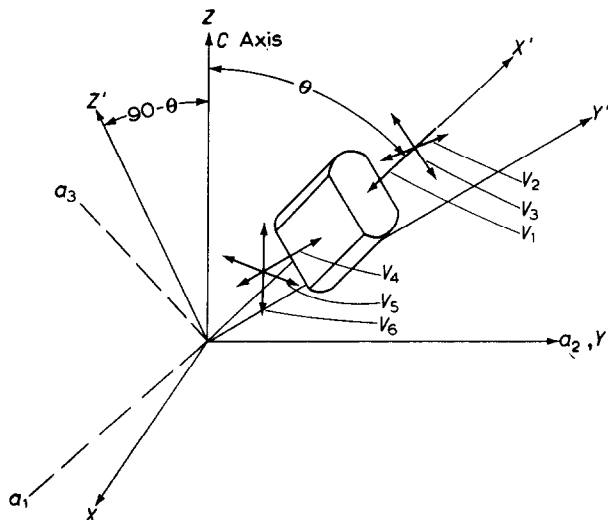


FIG. 2. Orientation of Mg crystals for measurements.

$XYZ$  are conventional stress-reference axes.

$X'Y'Z'$  are arbitrary stress-reference axes oriented with  $X'$  along the specimen axis, with  $Y'$  in the basal plane.

- $V_1$  is a longitudinal wave propagated along  $X'$ .
- $V_2$  is a shear wave propagated along  $X'$  with particle motion in the basal plane.
- $V_3$  is a shear wave propagated along  $X'$  with particle motion in the plane of the  $c$  axis.
- $V_4$  is a longitudinal wave propagated perpendicular to the  $c$  axis.
- $V_5$  is a shear wave propagated perpendicular to the  $c$  axis with particle motion in the basal plane.
- $V_6$  is a shear wave propagated perpendicular to the  $c$  axis, with particle motion along the  $c$  axis.

longitudinal waves,  $Y$  cut for transverse) was attached to a plane face of the sample by means of a thin (2-micron) layer of phenyl salicylate. Samples were cut so that the path lengths between faces were on the order of  $\frac{3}{4}$  in., and the round trip transit time of an acoustic pulse in the sample was measured by means of a Du Mont 256-D A-R oscilloscope. The approximate transit times for longitudinal waves were 6  $\mu$ sec, whereas for shear waves they were on the order of 12  $\mu$ sec.

At the magnesium-quartz interface there is a distortion of the pulse shape arising from the acoustic impedance mismatch which gives rise to a so-called "transit-time correction." Part of this correction probably arises in the electronics of the measuring equipment and part in the acoustics of the reflection, but its existence is experimentally shown by Fig. 3. In practice it is evidenced by a measured transit time which is longer than the actual transit time. In order to obtain a value for this correction, an experiment was performed in which apparent velocities were measured as a function of specimen length. A pure magnesium crystal oriented at  $39^\circ$  with respect to the  $c$  axis was cut up into four pieces of different lengths,

and each piece was measured. If  $V_t$  is the true velocity in the crystal,  $V_a$  the measured, apparent velocity,  $\delta t$  the transit-time correction, and  $L$  the length of the crystal, it is easy to show that:

$$1/V_a = \delta t/2L + 1/V_t \quad (8)$$

Plotting  $1/V_a$  against  $1/(2L)$  for a series of shear and longitudinal measurements, the graphs shown in Fig. 3 are obtained. The slopes of these plots yield the following values for the transit-time correction:

For longitudinal waves  $\delta t = 0.15 \mu$ sec

For shear waves  $\delta t = 0.14 \mu$ sec

These values were assumed to hold for all subsequent longitudinal and shear wave measurements—a valid procedure, since magnesium is nearly isotropic. The uncertainty in these numbers does, of course, affect the uncertainty of the absolute value of the elastic constants of pure Mg, but the relative effect of alloying is unaffected.

It should also be mentioned that large quartz crystals which nearly covered the entire face of the sample were used for these measurements. This was found to be necessary in order to circumvent an effect found with small quartzes and presumed to arise in diffraction coupled with the large transit-time correction. Such an effect interfered with the reproducibility and measurability of the pulse echoes.

At least two different measurements of transit time were made for each wave, more if it appeared necessary in order to get a value for the velocity that was good to 0.2%. The densities were obtained in the manner described above and are felt to be quite good, so the final  $\rho V^2$  values should be accurate to 0.5%. The elastic constants have then a  $\frac{1}{2}\%$  accuracy for the directly determined  $C_{11}$ ,  $C_{44}$ , and  $(C_{11} - C_{12})/2$ , but about 1% in the case of  $C_{33}$  and  $C_{13}$ , which are determined indirectly.

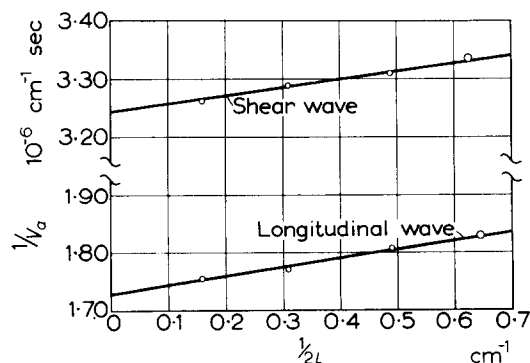


FIG. 3. Length experiment for establishing the magnitude of the "transit-time correction."

## RESULTS

The elastic constants obtained in this work for several pure magnesium crystals are listed in Table 1. The values are adiabatic and are for room temperature

TABLE 1. The adiabatic elastic constants of pure magnesium at 25°C from this work. Results are expressed in units of  $10^{12}$  dyne  $\text{cm}^{-2}$ . The value of  $C_{33}$  for crystal No. 5 is a direct determination, as are all the values of  $C_{11}$ ,  $C_{44}$ , and  $(C_{11} - C_{12})/2$  in the present work.

| Crystal No. | $C_{11}$ | $C_{33}$ | $C_{44}$ | $C_{12}$ | $C_{13}$ |
|-------------|----------|----------|----------|----------|----------|
| 3           | 0.5984   | 0.608    | 0.1636   | 0.2636   | 0.214    |
| 4           | 0.5941   | 0.617    | 0.1649   | 0.2587   | 0.217    |
| 5           |          | 0.621    | 0.1644   |          |          |
| 7           | 0.5997   | 0.619    | 0.1628   | 0.2649   | 0.220    |
| Average     | 0.5974   | 0.617    | 0.1639   | 0.2624   | 0.217    |

of 25°C. The internal agreement is seen to be excellent, and consistent with the precision estimates of the previous section. The authors have full confidence in these results, particularly for those constants and combinations which are directly determined. Comparison with previous results is reserved for Table 2 and the following paragraphs.

The adiabatic and isothermal constants and compliances for pure magnesium from this work are shown in Table 2. The adiabatic compliances  $S_{ij}$  have been computed from the adiabatic constants  $C_{ij}$  by the use of the following relations for a hexagonal 5-constant crystal:  $S_{44} = C_{44}^{-1}$

$$S_{11} - S_{12} = (C_{11} - C_{12})^{-1}, \quad S_{11} + S_{12} = C_{33}C^{-1},$$

$$S_{33} = (C_{11} + C_{12})C^{-1}, \quad S_{13} = -C_{13}C^{-1}$$

where  $C = C_{33}(C_{11} + C_{12}) - 2C_{13}^2$ .

The adiabatic compliances have been corrected to isothermal conditions by means of the thermodynamic expression,

$$S_{ij}^T - S_{ij}^s = T\gamma_i\gamma_j C_p^{-1}, \quad (9)$$

where  $T$  is the absolute temperature, 298°K,  $C_p$  is the specific heat taken as 6.00 cal (mole deg) $^{-1}$ , and the  $\gamma$ 's are thermal expansion coefficients. The expansion coefficients of Goens and Schmid<sup>(6)</sup> agree well with several other determinations, and are, in units of  $10^{-6}$  deg $^{-1}$ ,  $\gamma_1 = \gamma_2 = 25.4$ ,  $\gamma_3 = 27.0$ , and  $\gamma_4 = \gamma_5 = \gamma_6 = 0$ . The isothermal constants have then been computed from the isothermal compliances, using the conversion relations listed above with the  $C$ 's and  $S$ 's interchanged.

Finally, in Table 2 is listed in parentheses for comparison the adiabatic compliances of Goens and Schmid.<sup>(6)</sup> These values are taken from the last of a series of papers by these workers, and are quoted in this way, since their experimental method was an

TABLE 2. The values at 25°C for pure magnesium of the measured average adiabatic elastic constants  $C^s$ , the computed adiabatic compliances  $S^s$ , the isothermal compliances  $S^T$ , and the isothermal constants  $C^T$ . Units are  $10^{12}$  dyne  $\text{cm}^{-2}$  for  $C$  and  $10^{-12}$  cm $^2$  dyne $^{-1}$  for  $S$ . The values in parentheses are the measured values of Goens and Schmid<sup>6</sup> at "room temperature," which is inferred to be 20°C

| Term sub-script | $C^s$  | $S^s$              | $S^T$  | $C^T$  |
|-----------------|--------|--------------------|--------|--------|
| 11              | 0.5974 | 2.200<br>(2.215)   | 2.210  | 0.5852 |
| 12              | 0.2624 | -0.786<br>(-0.77)  | -0.775 | 0.2502 |
| 13              | 0.217  | -0.497<br>(-0.493) | -0.486 | 0.205  |
| 33              | 0.617  | 1.971<br>(1.975)   | 1.983  | 0.605  |
| 44              | 0.1639 | 6.101<br>(6.03)    | 6.101  | 0.1639 |

adiabatic  $S$  method in contrast to our adiabatic  $C$  method. Thus the adiabatic compliances are their direct result and the comparison is as fair as possible. It is also extremely favorable, the differences being about 1%, some of which could be in the probable temperature difference of 5°. Another independent determination of magnesium in the literature is that of Bridgman.<sup>(7)</sup> We have not made this comparison, which is poor, because Bridgman's method was a combination of static bending and torsion, and hydrostatic compression, and our experience leads us to distrust static methods with magnesium. Furthermore, Bridgman's result is that magnesium is isotropic, which is certainly not the case, as several direct determinations here show.

A severe test of any dynamic method of determining the elastic constants, and especially of the present  $C$  method, is to compare the computed compressibility with values directly measured by hydrostatic pressure. For magnesium the isothermal linear compressibilities  $k(c) = S_{33} + 2S_{13}$  and  $k(a) = S_{11} + S_{12} + S_{13}$ , expressed in units of  $10^{-12}$  cm $^2$  dyne $^{-1}$ , are: this paper, 1.011, 0.949; Bridgman,<sup>(7)</sup> 1.004, 1.004; Ebert,<sup>(8)</sup> 0.985, 1.000. Note that Ebert's values show the opposite anisotropy from the present ones and that Bridgman's 30°C values here quoted are isotropic. It is worth observing that, on the other hand, Bridgman's 75°C values show a 5% difference in the same sense as ours. Also in a later paper in which the same magnesium crystals were carried to a higher pressure,<sup>(9)</sup> the anisotropy appears to be about 2% in our sense,  $k(c) > k(a)$ , although actual compressibilities are not quoted. All in all, the writers are well satisfied with this comparison.

Table 3 lists the adiabatic elastic constants at 25°C for the alloy crystals which were grown and measured

TABLE 3. Measured values of the adiabatic elastic constants of magnesium alloys at 25°C. Results are expressed in units of  $10^{12}$  dyne  $\text{cm}^{-2}$ .

| Alloys atom % | Electron-atom ratio | $C_{11}$ | $C_{33}$ | $C_{44}$ | $C_{12}$ | $C_{13}$ |
|---------------|---------------------|----------|----------|----------|----------|----------|
| pure Mg       | 2.0000              | 0.5974   | 0.617    | 0.1639   | 0.2624   | 0.217    |
| 0.07% Ag      | 1.9993              | 0.5950   | 0.629    | 0.1640   | 0.2614   | 0.221    |
| 0.26% Ag      | 1.9974              | 0.6020   | 0.620    | 0.1664   | 0.2674   | 0.221    |
| 0.37% Ag      | 1.9963              | 0.5969   | 0.617    | 0.1640   | 0.2615   | 0.217    |
| 0.21% Sn      | 2.0042              | 0.5972   | 0.624    | 0.1630   | 0.2636   | 0.222    |
| 0.27% Sn      | 2.0054              | 0.5948   | 0.620    | 0.1638   | 0.2608   | 0.220    |
| 0.43% Sn      | 2.0086              | 0.5981   | 0.624    | 0.1632   | 0.2635   | 0.224    |
| 0.52% Sn      | 2.0104              | 0.5945   | 0.620    | 0.1621   | 0.2625   | 0.220    |
| 0.72% Sn      | 2.0144              | 0.5988   | 0.613    | 0.1623   | 0.2666   | 0.220    |
| 1.00% Sn      | 2.0200              | 0.5982   | 0.612    | 0.1610   | 0.2694   | 0.222    |
| 0.83% In      | 2.0083              | 0.5932   | 0.635    | 0.1620   | 0.2618   | 0.218    |
| 1.96% In      | 2.0196              | 0.5974   | 0.622    | 0.1613   | 0.2642   | 0.227    |

along with the chemical composition and the computed electron-atom ratio.

In Figs. 4, 5, and 6, the alloy results are presented in graphical form plotted against the electron-atom ratio. Rather than plotting the constants as tabulated, however, some important combinations representing certain crystallographically simple strain systems are used.  $C_{44}$  is the shear stress per unit shear strain required to change the angle between the  $c$  and  $a$  axes.  $(C_{11} - C_{12})/2$  is similar, except applying to the angle between any two orthogonal axes in the basal plane.  $(C_{11} + C_{12} + 2C_{33} - 4C_{13})$  is a combination corresponding to a strain  $\epsilon$  such that unit distance along the  $c$  axis becomes  $(1 + \epsilon)$  and unit distances in all directions in the basal plane become  $(1 + \epsilon)^{-1/2}$ . This combination of constants is then the second derivative of the energy with respect to  $\epsilon$ . Although this combination is not simply given by a wave velocity, it is very closely related to another constant, namely  $(C_{11} - C_{13})/2 + (C_{33} - C_{13})/2$ , which is measured nearly directly in these experiments by  $\rho V_3^2$ . The latter combination is roughly the ratio of shear stress to shear strain for a strain system comprising a compression along an  $a$  axis and an equal extension along the  $c$  axis.  $C_{33}$  is the ratio of normal stress to normal strain for compression along the  $c$  axis, with all other strains zero.  $C_{11}$  is analogous for pure compression along any direction in the basal plane.

In all of these graphs, the radii of the circles representing experimental points correspond to the estimated accuracies of the determinations. For pure Mg the average is shown together with the range of values given in Table 1. It may be seen that in all of these plots a straight line may be drawn which passes through almost all of the circles. The value of  $C_{33}$  for the 0.83 at. per cent indium alloy is out of line with the other measurements, but a careful check of the

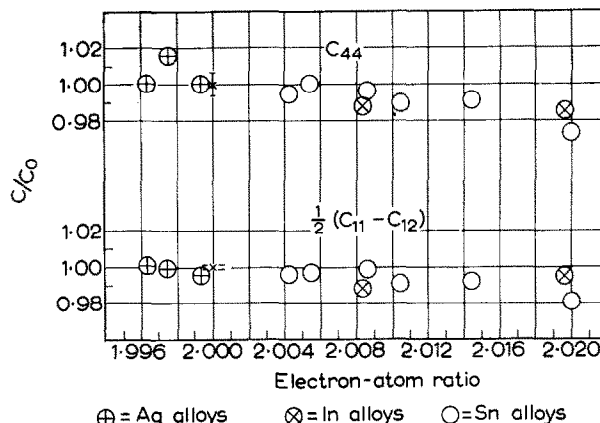


FIG. 4. The elastic constants  $C_{44}$  and  $(C_{11} - C_{12})/2$  for magnesium alloys versus electron-atom ratio.

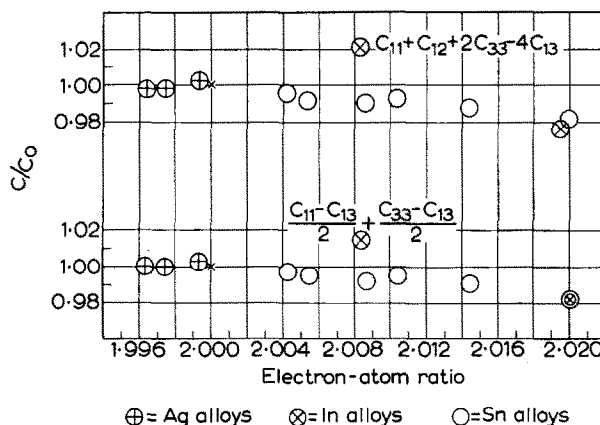


FIG. 5. The combinations  $C_{11} + C_{12} + 2C_{33} - 4C_{13}$  and  $(C_{11} - C_{13})/2 + (C_{33} - C_{13})/2$  for magnesium alloys versus electron-atom ratio.

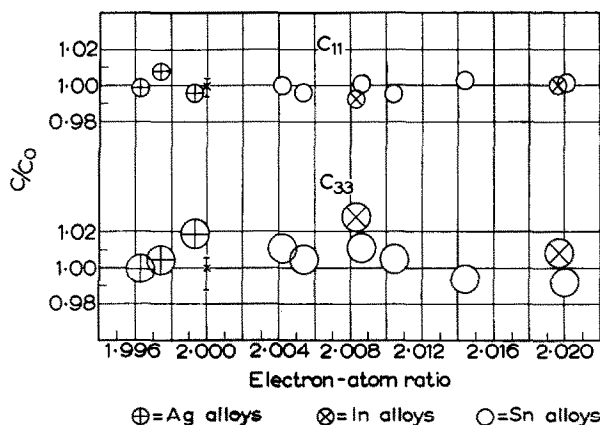


FIG. 6. The constants  $C_{11}$  and  $C_{33}$  for magnesium alloys versus electron-atom ratio.  $C_{11}$  is directly determined in this work, while  $C_{33}$  is not.

TABLE 4. The theoretical electrostatic and ion core contributions to the elastic constants of magnesium as calculated by Huntington<sup>(11)</sup>, compared with the experimental values at 25°C from this paper. Units are  $10^{12}$  dyne  $\text{cm}^{-2}$ .

| Constant                              | Electrostatic term | Ion core term | Sum   | Experimental |
|---------------------------------------|--------------------|---------------|-------|--------------|
| $C_{11} + C_{12} + 2C_{33} - 4C_{13}$ | 2.55               | 0.047         | 2.60  | 1.226        |
| $C_{11} - C_{12}$                     | 0.594              | 0.011         | 0.605 | 0.335        |
| $C_{44}$                              | 0.162              | 0.003         | 0.165 | 0.164        |

data fails to rectify the situation. The value obtained is just high.

### DISCUSSION

The shear constants for copper and some of the alkali metals have been calculated by Fuchs<sup>(10)</sup> in a treatment taking account of the change of electrostatic and ion-core energy as the crystal is strained. Since the free-electron picture fits these metals fairly well, the Fermi energy, correlation, and exchange energy should have negligible contributions under constant volume strain. Such a simple picture is not applicable to Mg with a nearly full zone, but it is of interest to see to what extent such a view does account for the shear constants in this hexagonal metal. Huntington<sup>(11)</sup> has made such a calculation, using the Ewald method to obtain the electrostatic potential energy at a lattice site and the Born-Mayer formula with modified Goldschmidt's ionic radii for a rough estimate of the ion-core term. The results of his calculation are shown in Table 4 along with the corresponding experimental numbers from this paper.

It is seen that the electrostatic term much more than accounts for the first two of these constants, which is at first surprising, since Fermi energy contributions have not been included in the theory. However, the electrostatic term can with good reason<sup>(3)</sup> be reduced from Huntington's result, and it would appear possible for the Fermi term to be negative for certain of the individual constants.<sup>(3)</sup> Detailed calculations for magnesium by our colleague J. R. Reitz are under way; pending their completion, further discussion will be confined to the effect of alloying.

A theory of elastic constants involving a detailed treatment of the Fermi energy contributions is that for aluminum by Leigh.<sup>(3)</sup> Leigh also calculates the behavior of the Fermi shear stiffnesses as the electron concentration is altered in alloying aluminum with a divalent metal. The predicted course of the two shear constants  $C_{44}$  and  $(C_{11} - C_{12})/2$  is shown in Fig. 7. Although Leigh treats a trivalent face-centered cubic metal, one can make some qualitative extensions of his discussion that apply to the behaviour of Mg with alloying.

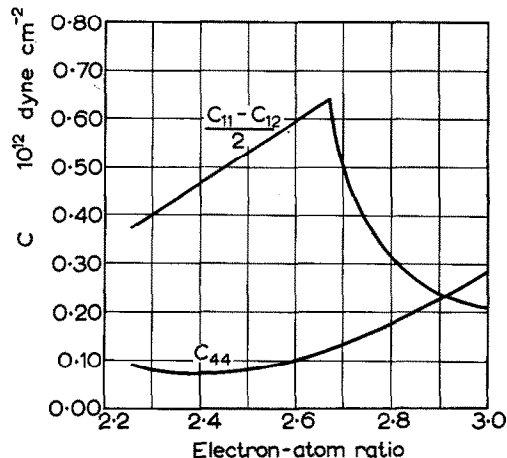


Fig. 7. Leigh's predictions for the variation of the elastic constants of aluminum with electron concentration.

Leigh considers the Fermi term to be composed of three parts: Contributions from a filled first zone, from overlapping electrons, and from holes in the first zone. A treatment of the filled first zone is a necessary device for obtaining the magnitude of the Fermi contribution; it yields a term which will not change with alloying.

There are two effects involved in the contributions from overlap electrons. Under shear, there is a shift of the overlap electron-energy surfaces with the zone faces as the Brillouin zone distorts, and there is also a transfer of electrons from those faces receding from the origin to those approaching it. The shift of energy surfaces with the faces yields a positive term in both the  $C_{44}$  and  $(C_{11} - C_{12})/2$  shears, while the transfer phenomenon results in larger, negative contributions in the two cases.

The effect of holes in the first zone is similar to that of overlapping electrons, except that their contribution from shifting as a whole with the zone faces is negative, whereas for electrons it was positive. The transfer of holes from one face to another is just the same as a transfer of electrons, so this still yields negative terms.

As the electron concentration is decreased in aluminum, electrons are first removed from their overlap positions over the square zone faces and thus the magnitude of the overlap transfer term is reduced. This results in less of a large negative contribution to  $(C_{11} - C_{12})/2$ , while  $C_{44}$  is only slightly affected, since only in a shear corresponding to the former constant are the square faces moved relative to the origin. This is essentially the reasoning which led Leigh to predict the behavior indicated in Fig. 7. It is to be noted that the most rapid decrease in  $(C_{11} - C_{12})/2$  with increasing electron concentration occurs very

suddenly at 2.67 electrons per atom, where overlap on the square faces is just initiated.

In magnesium, one might expect the same sort of behavior at an electron concentration of about 2.01 per atom, where other data indicate that overlap on the  $B$  faces in Fig. 1 has just occurred. This effect would be expected to show up in a shear which changed the relative distance of the  $B$  and  $A$  faces from the origin, because such a shear would produce a transfer of  $B$  overlap electrons to  $A$  faces presumably. A shear such as the one just described is the one corresponding to the elastic constant  $C_{11} + C_{12} + 2C_{33} - 4C_{13}$  shown in Fig. 5. Clearly, there is no sharp break in this constant as one passes through the critical region with alloying. This effect would also be expected in the accompanying constant plotted in Fig. 5. viz.  $(C_{11} - C_{33})/2 + (C_{33} - C_{13})/2$ . Since this latter constant is almost directly obtained in these experiments, the accuracy of this constant is good, the internal consistency of the measurements is high, and clearly no break is indicated.

It should be emphasized that a break such as shown in Fig. 7 for Al  $(C_{11} - C_{12})/2$  would be clearly seen on an experimental plot such as Fig. 5. The right-hand branch of the theoretical curve has infinite slope at the critical overlap concentration. On an experimental plot of discrete compositions and expanded scale such a characteristic would be exhibited practically as a discontinuity in the elastic constant from a point to the left of the cusp to one to the right. Such a discontinuity should be readily detected on an experimental plot even if the expected effect for magnesium is of smaller magnitude than for aluminum. At most, Fig. 5 exhibits a possible change in slope at the critical composition of 2.01 electron concentration. The data could be represented by a straight line of zero slope on the left and another of small negative slope on the right. But a slope change is a different matter from a discontinuity, and it must be concluded that a qualitative extension of the overlap theory from aluminum to magnesium is inadequate or that the overlap effect does not occur, at least under the present experimental conditions.

One would not expect, on the basis of Leigh's discussion, any pronounced effect in  $(C_{11} - C_{12})/2$  and  $C_{44}$  for Mg, and it is experimentally shown that these constants pass through the critical region smoothly.

Most of the constants show an overall fractional decrease upon alloying of about 1% per atomic per cent, somewhat less than the effect noticed in alloys

of Ag and Cu, where ion-core effects predominate.<sup>(12)</sup> The high indium composition point suggests that this decrease is primarily a function of the number of added electrons rather than of composition alone, but this point cannot be asserted because of the poor values obtained for the intermediate indium point. Lattice parameter changes account for no more than one-tenth the observed changes in elastic constant. It does not seem worthwhile to speculate on the reason for the trends shown, in view of the number of possible contributions to the elastic constants, of which many are of uncertain magnitude.

#### ACKNOWLEDGMENTS

This research was supported by the Office of Naval Research and the National Carbon Company. The authors are indebted to E. I. Salkovitz and A. I. Schindler for suggesting this problem and for numerous discussions of their own related work. Our colleague, J. R. Reitz, has helped greatly with the interpretation of the results. R. S. Busk and E. C. Burke of The Dow Chemical Company supplied the starting materials and gave much good advice on growing and handling the magnesium alloy crystals. We wish most sincerely to thank A. Hruschka for the staunch and patient support of his excellent machine-shop.

#### Note Added in Proof

Since the submission of this paper Reitz and Smith<sup>(13)</sup> have carried out a theoretical treatment of the elastic constants of magnesium and magnesium alloys in the nearly free electron approximation. The calculation is similar to that of Leigh<sup>(3)</sup> for aluminum. The elastic shear constants of magnesium can be accounted for, and when the effect of temperature is included the experimental alloy results can also be explained.

#### REFERENCES

1. A. I. SCHINDLER and E. I. SALKOVITZ *Phys. Rev.* **91**, 1320 (1953).
2. H. JONES *Proc. Roy. Soc. (London)* **A147**, 400 (1934).
3. R. S. LEIGH *Phil. Mag.* [7], **42**, 139 (1951).
4. J. R. NEIGHBOURS and C. S. SMITH *Acta Met.* **2**, 391 (1954).
5. J. R. NEIGHBOURS *J. Acoust. Soc. Amer.* **26**, 865 (1954).
6. E. GOENS and E. SCHMID *Physik. Zeits.* **37**, 385 (1936).
7. P. W. BRIDGMAN *Proc. Amer. Acad. Arts Sci.* **67**, 29 (1932).
8. H. EBERT *Physik. Zeits.* **36**, 385 (1935).
9. P. W. BRIDGMAN *Proc. Amer. Acad. Arts Sci.* **76**, 89 (1948).
10. K. FUCHS *Proc. Roy. Soc.* **A153**, 622 (1936).
11. H. B. HUNTINGTON *Phys. Rev.* **57**, 60 (1940), and by private communication.
12. R. BACON and C. S. SMITH *Acta Met.* **4**, 337 (1956).
13. J. R. REITZ and C. S. SMITH Scheduled for publication December 1 issue. *Phys. Rev.* **104** (1956).